

Wave packet dynamics in various two-dimensional systems: a unified description

Ashutosh Singh, Tutul Biswas, Tarun Kanti Ghosh, and Amit Agarwal*
Department of Physics, Indian Institute of Technology-Kanpur, Kanpur 208016, India
(Dated: January 7, 2018)

In this article we present an exact and unified description of wave-packet dynamics in various 2D systems in presence of a transverse magnetic field. We consider an initial minimum-uncertainty Gaussian wave-packet, and find that its long term dynamics displays the universal phenomena of spontaneous collapse and quantum revival. We estimate the timescales associated with these phenomena based on very general arguments for various materials, whose carrier dynamics is described either by the Schrödinger equation or by the Dirac equation.

PACS numbers: 03.65.Pm, 71.70.Di, 71.70.Ej, 72.80.Vp.

I. INTRODUCTION

Spontaneous collapse and consequent quantum revival [1,2] occurs in the long term dynamics of an injected wave-packet in systems with non-equidistant energy levels due to quantum interference. It has been investigated in a wide class of systems [3] and the phenomenon of wave packet collapse, revivals, and fractional revivals have been observed experimentally in a number of atomic and molecular systems [4–7]. However this phenomena of purely quantum mechanical in origin, is relatively less explored in condensed matter systems with discrete Landau energy levels, despite the fact that unlike *zitterbewegung* in solid state systems [8–10] these oscillations are large and slow enough for an experimental probe.

Zitterbewegung and wave-packet dynamics in several 2D condensed matter systems with Landau-levels have been explored earlier [10–16], but the phenomena of spontaneous collapse and revival has largely gone unaddressed [17–19]. Motivated by the unified description of *zitterbewegung* in solid state systems in Refs. [20,21], in this article we present an exact and unified description of the quantum wave-packet dynamics and the phenomena of collapse and quantum revival in various two dimensional (2D) solid state systems. Initially when a well localized wave packet is injected into a 2D system with non-equidistant Landau energy levels, it undergoes cyclotron motion and evolves quasi-classically with periodicity τ_{cl} , for a number of cycles, with its probability density spreading around the quasi-classical trajectory. Non-equidistant nature of the discrete energy spectrum then leads to destructive quantum interference and consequently the collapse of the wave-packet. The (almost) collapsed wave-packet regain their initial waveform and oscillate again with the quasi-classical periodicity on a much longer time scale known as revival time ($\tau_{rev} \gg \tau_{cl}$). In addition, there is also the possibility of fractional revivals which occurs at rational fraction of the revival time τ_{rev} when the initial wave-packet evolves into a collection of mini wave-packets resembling the waveform of the injected wave-packet [2,3].

In this article we consider several 2D systems, which can be classified into two categories based on the dynamics of the charge carriers: Schrödinger-like (non-

relativistic dynamics described by the Schrödinger equation) and Dirac-like fermionic systems [22] (relativistic dynamics described by the Dirac equation). The so called ‘Schrödinger-like’ materials include 2D electron/hole gas (2DEG/2DHG) trapped at the interface of III-V semiconductor hetero-structures, like AlGaAs-GaAs, and these typically have a linear [23,24] or cubic spin orbit interaction (SOI) terms [25–30] in addition to the parabolic dispersion relation. The so called ‘Dirac-like’ materials have a relativistic dispersion relation and typical examples include graphene [31–33] and other crystals like silicene [34–38], germanene [39,40], monolayer transition metal group-VI dichalcogenides MX_2 (M=Mo, W and X=S, Se) etc. [41–44] which generally have a honeycomb lattice structure. Dirac materials also have suppressed electron scattering and tunable electronic properties which make them very interesting from an application point of view.

For the present study, we consider both class of systems on an equal footing and present a unified and an exact description of quantum wave packet dynamics whose long term behavior displays the universal phenomena of spontaneous collapse and revival. For this purpose we choose the initial localized wave-packet to be a coherent state, which is also a minimum uncertainty wave packet, whose cyclotron dynamics resembles the dynamics of a classical charged particle in a perpendicular magnetic field [12].

Our article is organized as follows: In Sec. II we study the wave-packet dynamics in an exact and unified manner for various 2D systems with Landau levels. In addition we motivate and discuss the timescales associated with the phenomena of spontaneous collapse and revival in systems with discrete and non-equidistant energy levels. In Sec. III, we discuss the collapse and revival phenomenon in Schrödinger-like materials with parabolic energy spectrum and k -linear and k -cubic Rashba SOI. In Sec. IV we discuss wave-packet dynamics in Dirac-like materials with a relativistic dispersion, and finally, in Sec. V we summarize our results.

II. UNIFIED DESCRIPTION OF WAVE-PACKET DYNAMICS IN VARIOUS 2D SYSTEMS

In this section we present an exact and unified formalism describing the temporal evolution of a wave-packet in various 2D systems, in presence of a transverse magnetic field. In particular, we focus on both Schrödinger-like systems as well as Dirac-like materials, whose low energy properties are described by a two band model. In Sec. II A we calculate the exact expectation value of the position and velocity operator (or alternatively electric current), for an injected coherent state minimum uncertainty wave-packet in generic 2D systems. Next in Sec. II B, we briefly review the phenomenon of wave-packet revival in various 2D systems with Landau level spectrum.

A. Exact quantum evolution of a wave packet in various 2D systems

We begin by presenting an exact unified description of the temporal evolution of the center of an injected wave-packet in various two dimensional systems with non-equidistant Landau energy-levels. The Landau level eigen-spectrum describing different 2D systems can be written in the following generic form:

$$\varepsilon_n = \hbar\omega_c \left[f(n) + \lambda \sqrt{c^2 + g(n)} \right], \quad (1)$$

where $\lambda = \pm 1$ denotes two chiral energy branches, $f(n)$ and $g(n)$ are system dependent functions of the Landau level indexed by n , and c is a system dependent constant term. Note that $f(n)$ is generally a linear function of n in Schrödinger-like systems arising from the parabolic part of the dispersion relation, and it is generally absent in Dirac-like systems. The functions $f(n)$, $g(n)$ and c for various systems are tabulated in Table I. The magnetic length, for both class of systems, is given by $l_c = \sqrt{\hbar/(eB)}$. The cyclotron frequency, for Schrödinger-like systems is given by $\omega_c = eB/m^*$ with B being the applied transverse magnetic field and m^* is the effective mass. For Dirac-like systems $\omega_c = \sqrt{2}v_F/l_c$ where v_F is the Fermi velocity.

To specify the eigen-vectors, we assume the 2D system to lie in the $x - y$ plane and work in the Landau gauge, *i.e.* the vector potential is specified by $\mathbf{A} = (-By, 0, 0)$, where B is the strength of the magnetic field in the z -direction. The eigen-vectors corresponding to the eigen-energies given by Eq. (1) with different chiralities are now given by,

$$\psi_{n,q_x}^+(x, y) = \frac{e^{iq_x x}}{\sqrt{2\pi a_n}} \begin{pmatrix} -z_n \phi_{n-m}(y - y_c) \\ \phi_n(y - y_c) \end{pmatrix}, \quad (2)$$

and

$$\psi_{n,q_x}^-(x, y) = \frac{e^{iq_x x}}{\sqrt{2\pi a_n}} \begin{pmatrix} \phi_{n-m}(y - y_c) \\ z_n^* \phi_n(y - y_c) \end{pmatrix}, \quad (3)$$

TABLE I: Landau level of various 2D systems are given by Eq. (1), with the following:

System (Dispersion)	$f(n)$	c	$g(n)$
2DEG with linear Rashba	n	$\frac{g^* m^*}{4m_e} - \frac{1}{2}$	$\frac{2\alpha_1^2 n}{\hbar^2 \omega_c^2 l_c^2}$
2DHG with cubic Rashba	$n - 1$	$\frac{3g^* m^*}{4m_e} - \frac{3}{2}$	$\frac{8\alpha_3^2 n(n-1)(n-2)}{l_c^6 \hbar^2 \omega_c^2}$
Massive Dirac spectrum	0	$\Delta/(\hbar\omega_c)$	n

where m is an integer which depends on the related system, $|z_n| = \sqrt{g(n)/(c + \sqrt{c^2 + g(n)})}$, $a_n = 1 + |z_n|^2$ and $\phi_n(y - y_c) = N_n e^{-(y-y_c)^2/2l_c^2} H_n((y - y_c)/l_c)$ is the harmonic oscillator wave function. Other constants are given by $N_n = \sqrt{1/(\sqrt{\pi} 2^n n! l_c)}$, $y_c = q_x l_c^2$ and $H_n(x)$ denotes the Hermite polynomial of order n , and $z_n = |z_n|$ for Dirac-like materials and $z_n = i|z_n|$ for Schrödinger-like systems (within the chosen gauge). Note that the eigen-system described in Eqs. (1)-(3) is applicable only for $n \geq m$. For $n < m$ there are m Landau levels of ‘+’ chirality with eigen-energy $\varepsilon'_n = [f(n) - c]\hbar\omega_c$, and the corresponding two component eigen-vector is given by

$$\psi_n(\mathbf{r}) = \frac{e^{iq_x x}}{\sqrt{2\pi}} \begin{pmatrix} 0 \\ \phi_n(y - y_c) \end{pmatrix}. \quad (4)$$

Having described the generic form of Landau-levels and the associated eigen-vectors, in various 2D systems with two-bands, we now turn our attention to the dynamics of an injected wave-packet. For this purpose, we choose an initial wave-packet to be a coherent state in a magnetic field, *i.e.*, a Gaussian wave packet of the following form,

$$\Psi(\mathbf{r}, 0) = \exp\left(-\frac{r^2}{2l_c^2} + iq_0 x\right) \frac{1}{\sqrt{\pi} l_c \sqrt{|c_1|^2 + |c_2|^2}} \begin{pmatrix} c_1 \\ c_2 \end{pmatrix}, \quad (5)$$

where $\hbar q_0$ is the initial momentum along the x direction and the width of the Gaussian wave packet is considered to be equal to the magnetic length l_c , and the coefficients c_1 and c_2 determine the initial spin/pseudospin polarization of the injected wave-packet. The idea here is to choose a minimum uncertainty wave packet, whose cyclotron dynamics should resemble the dynamics of a classical particle in a perpendicular magnetic field. In addition such a wave-packet, when expressed in terms of Landau level eigen-states, is peaked around the Landau-level $n_0 \approx l_c^2 q_0^2 / 2$ (see for example, the Appendix A of Ref. [18]), and has a spread given by $\delta n = \sqrt{n_0}$.

We note here that such a simplistic choice of the initially injected wave-packet in Eq. (5), is widely used in the literature [12], is amenable to analytical treatment, and gives valuable insight into the relevant timescales of the problem. Another realistic experimental possibility is to create wave-packets by illuminating samples with short laser pulses [45].

The spinor wave packet at a later time t can be written

as

$$\Psi_\mu = \int G_{\mu\nu}(\mathbf{r}, \mathbf{r}', t) \Psi_\nu(\mathbf{r}', 0) d\mathbf{r}' , \quad (6)$$

where $G(\mathbf{r}, \mathbf{r}', t)$ is the 2×2 Green's function matrix. The matrix elements of the Green's functions are defined as [12]

$$G_{\mu\nu}(\mathbf{r}, \mathbf{r}', t) = \sum_{n,\lambda} \int dq_x \psi_{n,q_x,\mu}^\lambda(\mathbf{r}, t) \psi_{n,q_x,\nu}^{\lambda*}(\mathbf{r}', 0), \quad (7)$$

where $\psi_{n,q_x}^\lambda(\mathbf{r}, 0)$ is the two component spinor eigenfunctions at $t = 0$, given by Eqs. (2)-(3). At finite time, $\psi_{n,q_x}^\lambda(\mathbf{r}, t) = \psi_{n,q_x}^\lambda(\mathbf{r}, 0) e^{-i\epsilon_n^\lambda t/\hbar}$, with ϵ_n^λ being the Landau-level energy eigen-value given in Eq. (1).

Slightly lengthy but straightforward algebra gives the components of the Green's function matrix, to be of the following form,

$$G_{\mu\nu}(\mathbf{r}, \mathbf{r}', t) = \frac{1}{2\pi} \int_{-\infty}^{+\infty} dq_x e^{iq_x(x-x')} \eta_{\mu\nu}(q_x), \quad (8)$$

where $\eta_{\mu\nu}$ is given by

$$\eta_{11} = \sum_{n=0}^{\infty} P_{n+m} \phi_n(y - y_c) \phi_n(y' - y_c), \quad (9)$$

$$\eta_{21} = \sum_{n=0}^{\infty} Q_{n+m} \phi_{n+m}(y - y_c) \phi_n(y' - y_c), \quad (10)$$

$$\eta_{12} = \sum_{n=0}^{\infty} R_{n+m} \phi_n(y - y_c) \phi_{n+m}(y' - y_c), \quad (11)$$

$$\eta_{22} = \sum_{n=0}^{\infty} S_n \phi_n(y - y_c) \phi_n(y' - y_c), \quad (12)$$

and we have defined $\gamma_n \equiv \omega_c \sqrt{c^2 + g(n)}$, along with

$$P_n = e^{-if(n)\omega_c t} [e^{-i\gamma_n t} + 2i \sin(\gamma_n t)/a_n], \quad (13)$$

$$Q_n = 2iz_n^* e^{-if(n)\omega_c t} \sin(\gamma_n t)/a_n, \quad (14)$$

$$R_n = 2iz_n e^{-if(n)\omega_c t} \sin(\gamma_n t)/a_n, \quad (15)$$

$$S_n = \begin{cases} e^{-i\epsilon_n' t/\hbar} & \text{for } n < m \\ e^{-if(n)\omega_c t} [e^{i\gamma_n t} - 2i \sin(\gamma_n t)/a_n] & \text{for } n \geq m. \end{cases} \quad (16)$$

Substituting Eqs. (8)-(16) in Eq. (6), we obtain the time evolved two component injected wave packet at a later time t ,

$$\begin{pmatrix} \Psi_1(\mathbf{r}, t) \\ \Psi_2(\mathbf{r}, t) \end{pmatrix} = \frac{1}{\sqrt{2\pi}l_c} \int du e^{F(x,u)} \sum_{n=0}^{\infty} (-u)^n \frac{1}{\sqrt{c_1^2 + c_2^2}} \quad (17)$$

$$\times \left(\begin{pmatrix} c_1 P_{n+m} + \frac{c_2 (-u)^m R_{n+m}}{2^{n+m} (n+m)! N_{n+m}} \\ \frac{c_1 Q_{n+m} \phi_{n+m}(y-y_c) + c_2 S_n \phi_n(y-y_c)}{2^n n! N_n} \end{pmatrix} \phi_n(y - y_c) \right),$$

where $F(x, u) = iux/l_c - (l_c q_0 - u)^2/2 - u^2/4$ with $u = q_x l_c$ and $\hbar q_0$ is the momentum of the injected wave-packet. We emphasize that Eq. (17) gives the exact temporal evolution of the coherent state injected wave function with arbitrary spin/pseudo-spin polarization, for a wide-class of 2D materials.

In the rest of the paper we will focus on the specific case when the lower component of initial wave-packet is equal to zero, *i.e.*, the parameters $c_1 = 1$ and $c_2 = 0$ in Eq. (5). Now, the expectation value of the position operator $\hat{\mathbf{r}}$ (or any other operator), at time t , is simply given by

$$\langle \mathbf{r}(t) \rangle = \sum_{i=1}^2 \int \Psi_i^*(\mathbf{r}, t) \hat{\mathbf{r}} \Psi_i(\mathbf{r}, t) d\mathbf{r}. \quad (18)$$

A tedious but straightforward calculation using Eq. (17) in Eq. (18), gives us the exact time dependent expectation values of the position (x, y) , of the centre of the injected wave-packet to be

$$\begin{aligned} \langle x(t) \rangle &= l_c \sum_{n=0}^{\infty} \xi_n \left(\text{Im} [P_{n+m+1}(t) P_{n+m}^*(t)] \right. \\ &\quad \left. + \text{Im} [Q_{n+m+1}(t) Q_{n+m}^*(t)] \sqrt{\frac{n+m+1}{n+1}} \right), \end{aligned} \quad (19)$$

and

$$\begin{aligned} \langle y(t) \rangle &= l_c \sum_{n=0}^{\infty} \xi_n \left(\text{Re} [P_{n+m+1}(t) P_{n+m}^*(t)] \right. \\ &\quad \left. + \text{Re} [Q_{n+m+1}(t) Q_{n+m}^*(t)] \sqrt{\frac{n+m+1}{n+1}} - 1 \right), \end{aligned} \quad (20)$$

where we have defined

$$\xi_n \equiv \frac{i}{3} e^{-\frac{\tilde{q}_0^2}{3}} \left(\frac{-1}{12} \right)^n \frac{1}{n!} H_{2n+1} \left(i \sqrt{\frac{2}{3}} \tilde{q}_0 \right), \quad (21)$$

with $\tilde{q} = q_0 l_c$. Note that ξ_n is always real.

The temporal evolution of an incident wave-packet which is centered around some high energy level, in systems with discrete but non equidistant energy levels, typically displays the phenomena of spontaneous collapse and revival [3]. However it is generally difficult to infer the relevant timescales associated with these phenomena, from the exact expressions for the position operators given in Eqs. (19)-(20). Thus we briefly discuss the phenomena of spontaneous collapse and revival, based on general arguments in the next subsection. Later, in Sec. III and Sec. IV, we will show the emergence of these timescales from the exact solution in various 2D systems.

B. Oscillation, cyclotron and revival timescales

Discretized Landau energy-levels are formed whenever a 2D electronic system, is subjected to a strong per-

pendicular magnetic field. The spatio-temporal evolution of wave-packets in such quantum system with discrete but non-equidistant energy spectrum is generally quiet complex and exhibits both classical and quantum behavior. The quantum behavior being manifested in the form of spontaneous collapse and long term quantum revival of the wave-packet arising due to quantum interference. However well defined periodicities for quasi-classical behavior, spontaneous collapse and revival emerge [3,17,46,47], if the initial wave packet have a substantial overlap with some large Landau level denoted by n_0 .

Various timescales during the wave packet dynamics in a discrete system with non-equidistant energy spectrum, can be inferred from the analytic form of the autocorrelation function [46] of the wave packet, which is defined as $A(t) = \langle \Phi(\mathbf{r}, t) | \Phi(\mathbf{r}, 0) \rangle$. Expanding $\Phi(\mathbf{r}, t)$ in terms of the orthonormal eigenstates of the system under consideration, $\{\phi_n\}$, we get $\Phi(\mathbf{r}, t) = \sum_n c_n \phi_n(\mathbf{r}) e^{-i\epsilon_n t/\hbar}$, where ϵ_n are the discrete energy eigenvalues of the system and $c_n = \langle \phi_n(\mathbf{r}) | \Phi(\mathbf{r}, 0) \rangle$. The autocorrelation function is now given by

$$A(t) = \sum_n |c_n|^2 e^{i\epsilon_n t/\hbar}. \quad (22)$$

For studying the dynamics of a localized injected wave packets, which can be expressed as a superposition of the eigen-states of the system centered around some large Landau-level $n = n_0$, such that $n_0 \gg \delta n \gg 1$, we can assume the form of the expansion coefficients to a Gaussian centered around n_0 with spread of δn . Doing a Taylor series expansion of the energy, $\epsilon_n = \epsilon_{n_0} + (n - n_0)\epsilon'_{n_0} + (n - n_0)^2 \epsilon''_{n_0}/2 + \dots$, where $\epsilon'_n = (d\epsilon_n/dn)_{n=n_0}$ and so forth, the autocorrelation function can be rewritten as,

$$A(t) = \sum_{n=-\infty}^{\infty} |c_n|^2 e^{it/\hbar(\epsilon_{n_0} + (n-n_0)\epsilon'_{n_0} + (n-n_0)^2 \epsilon''_{n_0}/2 + \dots)}. \quad (23)$$

The coefficients of the Taylor expansion of the energy ϵ_n in the exponential of Eq. (23) defines a characteristic timescale via,

$$\tau_{\text{osc}} = \frac{2\pi\hbar}{\epsilon_{n_0}}, \quad \tau_{\text{cl}} = \frac{2\pi\hbar}{|\epsilon'_{n_0}|}, \quad \text{and} \quad \tau_{\text{rev}} = \frac{4\pi\hbar}{|\epsilon''_{n_0}|}. \quad (24)$$

The timescale τ_{osc} , is an intrinsic quantum oscillation time scale, which does not lead to any quantum interference in the various wave packet components of different Landau-levels and is thus it does not effect the long term dynamics of the system. At the ‘classical’ cyclotron time-scale τ_{cl} , the wave-packet evolves quasi-classically and the center of the wave-packet completes one cyclotron orbit, and returns to the initial position and the autocorrelation function approximately reaches its initial value.

At larger timescales quantum interference between the wave function components of different Landau levels in the incident wave-packet, leads to spontaneous collapse

of the wave function and then to quantum revival. The quantum revival of the wave packet, over timescale τ_{rev} , occurs due to constructive interference when the terms proportional to the second derivative in the energy are in multiples of 2π . This revival hierarchy sustains even in the higher order terms. In addition the time at which the spreading of the wave packet leads to quantum self-interference which leads to spontaneous collapse, is given by $\tau_{\text{coll}} = \tau_{\text{rev}}/(\delta n)^2$. See Ref. [3] for a detailed review.

For this article, where the generic Landau-level spectrum for various 2D systems is given by Eq. (1), corresponding derivatives of the energy with respect to n , which appear in Eq. (24) are explicitly given by

$$\frac{\epsilon'_n}{\hbar\omega_c} = f'(n) + \lambda \frac{g'(n)}{2\sqrt{c^2 + g(n)}}, \quad (25)$$

and

$$\frac{\epsilon''_n}{\hbar\omega_c} = f''(n) + \frac{\lambda}{2\sqrt{c^2 + g(n)}} \left[g''(n) - \frac{g'(n)^2}{2(c^2 + g(n))} \right], \quad (26)$$

where $f(n)$ is typically a linear function of n , arising from the parabolic part of the dispersion relation, which exists only for Schrödinger-like systems, and thus $f'(n)$ is a constant and $f''(n) = 0$.

The classical, spontaneous collapse and revival timescales for various 2D systems studied in this paper, along with the relevant material parameters, is tabulated in Table II and Table III. We now proceed to study the phenomena of revival and collapse in various systems like k -linear Rashba 2DEG, k -cubic rashba 2DHG etc.

III. SCHRÖDINGER-LIKE SYSTEMS

In this section we discuss spontaneous decay and long-term quantum revival of a quantum wave packet in two-dimensional Schrödinger-like fermionic systems described by Rashba spin-orbit interaction (SOI). Let us first consider the case of a 2DEG with k -linear Rashba SOI.

A. 2DEG with k -linear Rashba SOI

We now examine the wave-packet dynamics in a 2DEG formed at the interface of an *inversion asymmetric* III-V semiconductor quantum well, subjected to a Zeeman field perpendicular to the interface. The inversion asymmetry of the quantum well gives rise to Rashba SOI [48], which has a linear dependence on momentum.

To obtain the Landau level spectrum of a Rashba 2DEG in a transverse magnetic field, we work with Landau gauge $\mathbf{A} = (-By, 0, 0)$ for the vector potential. Making the Landau-Peierls substitution $\mathbf{p} \rightarrow \mathbf{\Pi} = \mathbf{p} + e\mathbf{A}/\hbar$, the Hamiltonian [49] describing Rashba 2DEG is given by

$$H = \frac{\mathbf{\Pi}^2}{2m^*} + \frac{\alpha_1}{\hbar} (\sigma_x \Pi_y - \sigma_y \Pi_x) + \frac{1}{2} g^* \mu_B \sigma_z B, \quad (27)$$

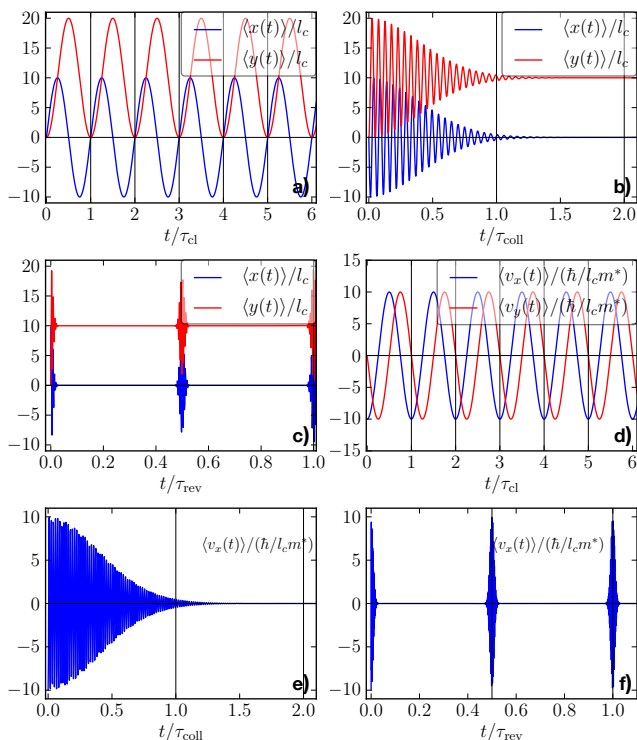


FIG. 1: Panel a), b), and c) show the position of the center of the wave packet vs time, while panels d), e) and f) display the velocity expectation value, over different timescales, *i.e.* τ_{cl} , τ_{coll} and τ_{rev} respectively. Note that in panels a), b) and c) $\langle x(t) \rangle$ is centered around 0, whereas $\langle y(t) \rangle$ is centered around $y_c = q_0 l_c^2 = 10$. Here we have chosen $B = 2\Gamma$ and other material parameters for AlGaAs/GaAs quantum well: $m^* = 0.067m_e$, $g^* = -0.44$, $\alpha_1 = 10^{-13}$ eV-m.

where m^* is the effective mass of the electron, α_1 is the Rashba SOI coupling coefficient, g^* is the effective Lande g -factor, μ_B is the Bohr magneton and σ_i denote the Pauli spin matrices. The Landau-level eigen-spectrum corresponding to Eq. (27) is given [49] by the generic form considered in Eq. (1) with the following substitutions:

$$f(n) = n, \quad c = \frac{g^* m^*}{4m_e} - \frac{1}{2}, \quad \text{and} \quad g(n) = \frac{2\alpha_1^2 n}{\hbar^2 \omega_c^2 l_c^2}, \quad (28)$$

where m_e is the free electron mass. The corresponding eigen-vectors for the two spin-split branches ($\lambda = \pm 1$) are now simply obtained by putting $m = 1$ in Eqs. (2)-(3).

Now the temporal evolution of the expectation value of the coordinates (x, y) of the centre of the injected Gaussian wave-packet are given by Eq. (19) and Eq. (20) with $m \rightarrow 1$. As a check of our calculation, we note that the expectation values of the position operator are consistent with that derived in Eqs. (36a)-(36b) of Ref. [12].

Let us now calculate the time-dependent expectation values of the velocity operator, which also gives the charge current. Using the Heisenberg equation of motion for the position operator, $\dot{\hat{\mathbf{v}}} = -i\hbar^{-1}[\hat{\mathbf{r}}, H]$, the compo-

nents of the velocity operator are given by

$$\hat{v}_x = \frac{\hat{\Pi}_x}{m^*} - \frac{\alpha_1}{\hbar} \sigma_y, \quad \text{and} \quad \hat{v}_y = \frac{\hat{\Pi}_y}{m^*} + \frac{\alpha_1}{\hbar} \sigma_x. \quad (29)$$

Following the same procedure as described in Sec. II A, we finally obtain the following expressions for the components of the velocity expectation values,

$$\begin{pmatrix} \langle v_x(t) \rangle \\ \langle v_y(t) \rangle \end{pmatrix} = \frac{\hbar}{l_c m^*} \sum_{n=0}^{\infty} \xi_n \begin{pmatrix} \text{Re } v_n \\ \text{Im } v_n \end{pmatrix}, \quad (30)$$

where we have defined

$$v_n \equiv P_{n+2}^* P_{n+1} + Q_{n+2}^* Q_{n+1} \sqrt{\frac{n+2}{n+1}} + \frac{i\tilde{\alpha}_1}{\sqrt{n+1}} P_{n+2}^* Q_{n+1}, \quad (31)$$

using the dimensionless SOI strength: $\tilde{\alpha}_1 = \sqrt{2}\alpha_1/(l_c \hbar \omega_c)$ and ξ_n is defined in Eq. (21).

To discuss wave-packet dynamics which shows the phenomena of spontaneous collapse and revival, we compute the relevant time scales described in Sec. II B for 2DEG with k -linear Rashba SOI. The oscillation, classical and quantum revival timescales for this system are respectively given by

$$\tau_{osc}^\lambda = \tau_c \frac{1}{|n_0 + \lambda \sqrt{c^2 + \tilde{\alpha}_1^2 n_0}|}, \quad (32)$$

$$\tau_{cl}^\lambda = \tau_c \frac{1}{|1 + \lambda \frac{\tilde{\alpha}_1^2}{2\sqrt{c^2 + \tilde{\alpha}_1^2 n_0}}|}, \quad (33)$$

and finally,

$$\tau_{rev} = \tau_c \frac{8[c^2 + \tilde{\alpha}_1^2 n_0]^{3/2}}{\tilde{\alpha}_1^4}, \quad (34)$$

where $\tau_c = 2\pi/\omega_c$. Note that there are two contributions in τ_{osc} and τ_{cl} coming from the upper and lower branches of the energy spectrum. In the rest of the paper, we will be using the average timescales defined as $\tau_{osc} = (\tau_{osc}^+ + \tau_{osc}^-)/2$ and $\tau_{cl} = (\tau_{cl}^+ + \tau_{cl}^-)/2$.

Experimentally, k -linear Rashba SOC is present in an AlGaAs/GaAs quantum well [23] or in an InGaAs/InAlAs quantum well [24] among other materials. Various parameters and the corresponding timescales for these are given in Table. II. We study the dynamics of the center of the wave-packet and its velocity (or equivalently current), in Fig. 1, using the material parameters of an AlGaAs/GaAs quantum well. Both the position and velocity of an initial minimum-uncertainty wave-packet display the phenomena of spontaneous collapse and consequent full quantum revival at long times.

B. 2D systems with k -cubic Rashba SOI

In this section we investigate the wave-packet dynamics in 2DEG and 2DHG with parabolic dispersion relation

TABLE II: The parameters and associated timescales for various 2D Schrödinger-like systems. Here $n_0 = 50$ and $B = 2T$.

System	material (quantum well)	m^*/m_e	g^*	SOI: α_1 (eV-m) or α_3 (eV-m ³)	τ_{osc} (fs)	τ_{cl} (ps)	τ_{rev} (ns)
Systems with							
linear Rashba SOI	AlGaAs/GaAs ²³	0.067	-0.44	$\alpha_1 = 10^{-13}$	23.94	1.19	48.3×10^6
	InGaAs/InAlAs ²⁴	0.052	4.0	$\alpha_1 = 10^{-11}$	18.59	0.93	18.04
2DEG with							
cubic Rashba SOI	GaAs/AlGaAs (2DHG) ^{25,26,50}	0.45	7.2	$\alpha_3 = 10^{-29}$	165	8.11	13.70
	SrTiO ₃ (2DEG) ^{29,30}	1.45	2.0	$\alpha_3 = 10^{-30}$	529	25.92	102.02

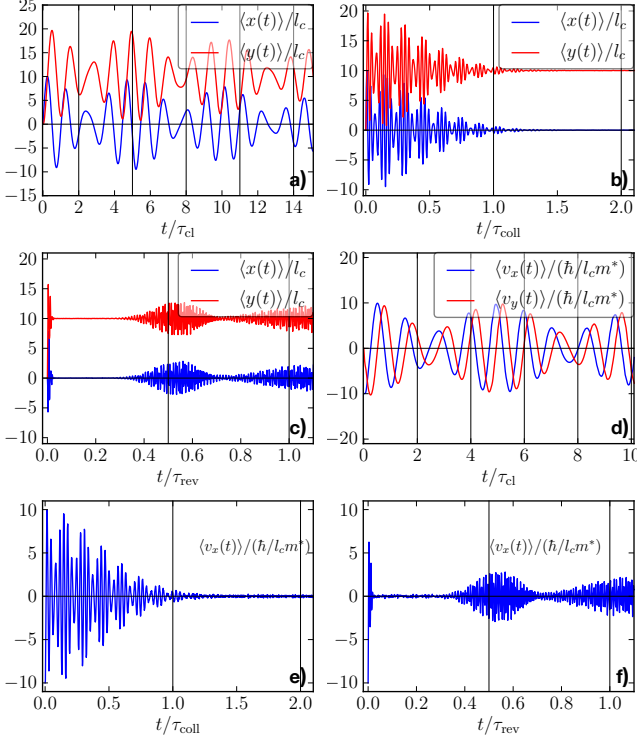


FIG. 2: As in Fig. 1, panels a), b), and c) show the position, and panels d), e), and f) show the velocity expectation vs time, for different timescales. Here we have chosen $B = 2T$ and other material parameters for 2D hole gas formed at p -type GaAs/AlGaAs heterostructure which are: $m^* = 0.45m_e$, $g^* = 7.2$, $\alpha_3 = 10^{-29}$ eV-m³.

along with the Rashba SOI which is cubic in momentum. Generally k -cubic Rashba SOI occurs in two different systems. One of such systems is 2D heavy hole gas [25–28,50] formed at the interface of p -doped III-V semiconductors, namely GaAs/AlGaAs heterostructure. In addition k -cubic Rashba SOI can also be found in the 2D electron gas formed at the interface of perovskite oxide structures [29,30,51] such as LaAlO₃/SrTiO₃ interface and SrTiO₃ surface.

The single particle Hamiltonian [52,53] of a 2D system with cubic Rashba SOI, in a transverse magnetic field is

given by

$$H = \frac{\mathbf{\Pi}^2}{2m^*} + \frac{i\alpha_3}{2\hbar^3} (\Pi_-^3 \sigma_+ - \Pi_+^3 \sigma_-) + \frac{3}{2} g_s \mu_B \boldsymbol{\sigma} \cdot \mathbf{B}, \quad (35)$$

where $\mathbf{\Pi}$ is the conjugate momentum defined in previous section, α_3 is the Rashba coupling coefficient. Additionally, we have defined $\Pi_{\pm} \equiv \Pi_x \pm i\Pi_y$, and $\sigma_{\pm} \equiv \sigma_x \pm i\sigma_y$. Note that for the case of heavy holes, the Pauli matrices represent an effective pseudo-spin with spin projection $\pm 3/2$ along the growth direction of the quantum well.

The Landau level spectrum is again given by Eq. (1), with

$$f(n) = n - 1, \quad g(n) = \frac{8\alpha_3^2 n(n-1)(n-2)}{l_c^6 \hbar^2 \omega_c^2}, \quad (36)$$

and finally

$$c = \frac{3g^* m^*}{4m_e} - \frac{3}{2}. \quad (37)$$

Similarly, the temporal evolution of the expectation values of the position operators for the centre of the wavepacket are given by substituting $m = 3$ in Eqs. (19)-(20). The components of the velocity operator are given by

$$\hat{v}_x = \frac{\Pi_x}{m^*} \sigma_0 + \frac{3i\alpha_3}{2\hbar^3} (\sigma_+ \Pi_-^2 - \sigma_- \Pi_+^2), \quad (38)$$

and

$$\hat{v}_y = \frac{\Pi_y}{m^*} \sigma_0 + \frac{3\alpha_3}{2\hbar^3} (\sigma_+ \Pi_-^2 + \sigma_- \Pi_+^2). \quad (39)$$

Their expectation values are given by

$$\begin{pmatrix} \langle v_x(t) \rangle \\ \langle v_y(t) \rangle \end{pmatrix} = \frac{\hbar}{l_c m^*} \sum_{n=0}^{\infty} \xi_n \begin{pmatrix} \text{Re } h_n \\ \text{Im } h_n \end{pmatrix}, \quad (40)$$

where we have defined

$$\begin{aligned} h_n &\equiv P_{n+4}^* P_{n+3} + \sqrt{\frac{n+4}{n+1}} Q_{n+4}^* Q_{n+3} \\ &+ 3i\tilde{\alpha}_3 \sqrt{\frac{(n+2)(n+3)}{n+1}} P_{n+4}^* Q_{n+3}, \end{aligned} \quad (41)$$

using the dimensionless SOI strength: $\tilde{\alpha}_3 = 2\sqrt{2}\alpha_3/(l_c^3 \hbar \omega_c)$ and ξ_n is defined in Eq. (21). Note that

the expectation values of the position and velocity operators for systems with k -cubic Rashba SOI have recently been reported in Ref. [15], and are presented here for completeness, and to emphasize that they can be derived from our unified description.

The oscillation, classical, and revival timescales are now given by,

$$\tau_{\text{osc}}^\lambda = \tau_c \frac{1}{|n_0 - 1 + \lambda \sqrt{c^2 + g(n_0)}|}, \quad (42)$$

$$\tau_{\text{cl}}^\lambda = \tau_c \frac{1}{|1 + \lambda \frac{\tilde{\alpha}_3^2(3n_0^2 - 6n_0 + 2)}{2\sqrt{c^2 + g(n_0)}}|}, \quad (43)$$

and

$$\tau_{\text{rev}} = \tau_c \frac{4\sqrt{c^2 + g(n_0)}}{\tilde{\alpha}_3^2 \left\{ 6(n_0 - 1) - \frac{\tilde{\alpha}_3^2}{2[c^2 + g(n_0)]} (3n_0^2 - 6n_0 + 2) \right\}}. \quad (44)$$

The phenomena of spontaneous collapse is evident in Fig. 2b and Fig. 2e for the position and the velocity of the centre of the injected wave-packet respectively. The phenomena of partial and full quantum revival in 2DHG is evident in Fig. 2c and Fig. 2f.

IV. DIRAC MATERIALS

In this section we focus on systems whose energy dispersion is similar to that given by the relativistic Dirac equation, such as graphene [31–33], silicene [34–38], monolayer group-VI dichalcogenides MX_2 (M=Mo, W and X=S, Se) etc [41–44]. The low-energy Hamiltonian describing these systems is simply given by,

$$H = v_F(p_x\sigma_x + p_y\sigma_y) + \Delta\sigma_z, \quad (45)$$

where v_F is the Fermi velocity, and 2Δ is the band gap, both of which differ from system to system (see Table III). If the band gap $\Delta \rightarrow 0$, then Eq. (45) describes massless Dirac fermions as in graphene. Typically, the band gap varies from 0 – 1 eV in these systems, and in silicene it can even be tuned experimentally by means of an externally applied electric field [40].

The effect of a transverse magnetic field is included by the usual Landau-Peierls substitution in Eq. (45). The Landau-Level eigen-spectrum is again given by the generic Eq. (1), after substituting

$$f(n) = 0, \quad g(n) = n, \quad \text{and} \quad c = \Delta/(\hbar\omega_c). \quad (46)$$

The corresponding Landau level wave-functions are given by Eqs. (2)-(3), with the substitution $m \rightarrow 1$.

The time-evolved injected wave-packet at a later time t can be obtained from Eq. (17), with $m = 1$. The coordinates of the center of the wave packet at later times are now given by the generic Eqs. (19)-(20) after the

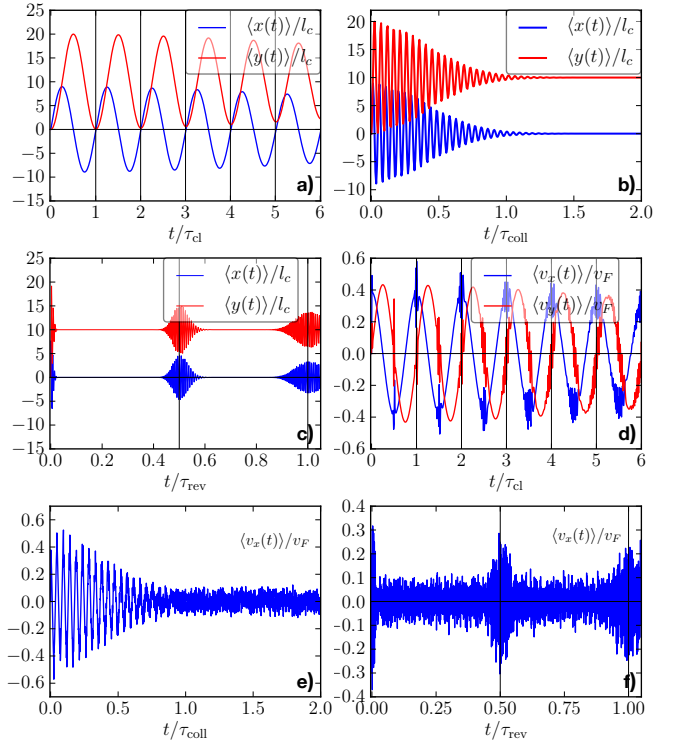


FIG. 3: As in Fig. 1, panels a), b), and c) show the position, and panels d), e), and f) show the velocity expectation vs time, for different timescales. Other parameters are $\Delta = 0.4\text{eV}$, $v_F = 532000 \text{ m/s}$, $B = 2\text{T}$ and $q_0l_c=10$.

substitution $m \rightarrow 1$. The velocity operator is given by the Heisenberg equation of motion: $\hbar\dot{v}_j = i[\hat{H}, \hat{r}_j]$, and straightforward calculations yield the following expressions for the expectation value for the velocity of the center of the injected wave-packet,

$$\langle v_x(t) \rangle = \text{Re} [\langle v(t) \rangle], \quad \text{and} \quad \langle v_y(t) \rangle = \text{Im} [\langle v(t) \rangle], \quad (47)$$

where

$$\langle v(t) \rangle = \sqrt{2}v_F \sum_{n=0}^{\infty} \xi_n \frac{1}{\sqrt{1+n}} P_{n+2}^* Q_{n+1}. \quad (48)$$

The oscillation, classical and revival timescales in this case are given by,

$$\tau_{\text{osc}} = \frac{2\pi\hbar}{\varepsilon_{n_0}}, \quad \tau_{\text{cl}} = \frac{4\pi\hbar\varepsilon_{n_0}}{\varepsilon^2}, \quad \text{and} \quad \tau_{\text{rev}} = \frac{16\pi\hbar\varepsilon_{n_0}^3}{\varepsilon^4}, \quad (49)$$

where $\varepsilon_{n_0} = \sqrt{\Delta^2 + \varepsilon^2 n_0}$ and $\varepsilon = \sqrt{2}\hbar v_F/l_c$.

We tabulate different materials, whose low energy properties are described by Eq. (45) in Table III, along with their material properties, and the relevant oscillation, classical and revival timescales. We plot the expectation value of the position and velocity of the center of the wave-packet in Fig. 3 over the classical, collapse

TABLE III: The parameters for various 2D Dirac-like materials and the associated time-scales. Here $n_0 = 50$ and $B = 2T$.

Material	Fermi velocity (10^6 ms^{-1})	Band Gap (eV)	τ_{osc} (fs)	τ_{cl} (ps)	τ_{rev} (ns)
Graphene ³¹⁻³³	1	Gapless	11.39	1.13	0.22
Silicene ³⁶⁻³⁸	0.532	0 - 0.2 (tunable)	21.4-19.02	2.14-2.41	0.42-0.61
Germanene ⁴⁰	0.517	0 - 0.2 (tunable)	22.0-19.4	2.2-2.5	0.44-0.64
MoS ₂ ^{41,43}	0.085	1.6	5.16	348.12	4.69×10^4

and revival timescales to highlight the the phenomena of spontaneous collapse and quantum revival.

Note that the value for band gap plays an important role in determining the relevant timescales. In particular the revival time for MoS₂ is quite large as compared to other Dirac-like materials due to its large band-gap. However the band-gap is not a fixed quantity, and in some materials it can be varied by the application of a transverse electric fields (as in silicene) or by doping (as in transition Metal dichalcogenides).

V. SUMMARY AND CONCLUSIONS

We present a unified treatment of wave-packet dynamics in various 2D systems, in presence of a transverse magnetic field, and the associated phenomena of spontaneous collapse and long term quantum revival of the wave-packet. In particular we focus on a minimum uncertainty Gaussian wave packet and obtain exact expressions for the expectation values of the position and velocity operators for a variety of 2D materials, in addition to the various timescales associated with the phenomena of spontaneous collapse and quantum revival.

For any system with discrete and non-equidistant Lan-

dau level spectrum injecting an initial electron wave packet which is peaked (centered) around some Landau level, we find that the wave packet initially evolves quasi-classically and oscillate with a period of τ_{cl} (the cyclotron time-period). However at larger times, the wave packet eventually spreads and quantum interference between the different Landau level components of the wave-function leads to its ‘collapse’, and at even longer times, that are multiples (or rational fractions) of τ_{rev} , quantum interference results in long-term revival of the wave packet, and the electron position and velocity regains its initial amplitude — again undergoing quasiclassical oscillatory motion.

To summarize finally, we present a unified and exact analytical treatment of wave-packet dynamics in various 2D spin-orbit coupled Schrödinger systems and Dirac-like materials. As expected on general grounds, for any system with phenomenon of spontaneous collapse and quantum revival.

Acknowledgements

A. A. gratefully acknowledges funding from the INSPIRE Faculty Award by DST (Govt. of India), and from the Faculty Initiation Grant by IIT Kanpur, India.

-
- * Electronic address: amitag@iitk.ac.in
- ¹ J. Parker, C. R. Stroud Jr., *Phys. Rev. Lett.* **56**, 716 (1986).
 - ² I. Sh. Averbukh and N. F. Perelman, *Phys. Lett. A* **139** 449 (1989).
 - ³ R. W. Robinett, *Phys. Rep.* **392**, 1 (2004).
 - ⁴ J. A. Yeazell, M. Mallalieu, and C. R. Stroud, Jr., *Phys. Rev. Lett.* **64**, 2007 (1990).
 - ⁵ J. A. Yeazell and C. R. Stroud, Jr., *Phys. Rev. A* **43**, 5153 (1991).
 - ⁶ D. R. Meacher, P. E. Meyler, I. G. Hughes, P. Ewart, *J. Phys. B* **24** L63 (1991).
 - ⁷ J. Wals, H. H. Fielding, J. F. Christian, L. C. Snoek, W. J. van der Zande, and H. B. van Linden van den Heuvell, *Phys. Rev. Lett.* **72**, 3783 (1994).
 - ⁸ W. Zawadzki, *Phys. Rev. B* **72**, 085217 (2005).
 - ⁹ J. Schliemann, D. Loss, and R. M. Westervelt, *Phys. Rev. Lett.* **94**, 206801 (2005); *Phys. Rev. B* **73**, 085323 (2006).
 - ¹⁰ W. Zawadzki and T. M. Rusin *J. Phys.: Condens. Matter* **23**, 143201 (2011).
 - ¹¹ T. M. Rusin and W. Zawadzki, *Phys. Rev. D* **82**, 125031 (2010).
 - ¹² V. Y. Demikhovskii, G. M. Maksimova, and E. V. Frolova, *Phys. Rev. B* **78**, 115401 (2008).
 - ¹³ T. M. Rusin and W. Zawadzki, *Phys. Rev. B* **78**, 125419 (2008).
 - ¹⁴ J. Schliemann, *New J. Phys.* **10**, 043024 (2008).
 - ¹⁵ T. Biswas and T. K. Ghosh, *J. Appl. Phys.* **115**, 213701 (2014).
 - ¹⁶ A. Singh, T. Biswas, T. K. Ghosh and A. Agarwal [arXiv:1404.4534](https://arxiv.org/abs/1404.4534) (2014).
 - ¹⁷ E. Romera and F. de los Santos, *Phys. Rev. B* **80**, 165416 (2009). T. Garcia, N. A. Cordero, and E. Romera, *Phys. Rev. B* **89**, 075416 (2014).
 - ¹⁸ V. Krueckl and T. Kramer, *New J. Phys.* **11**, 093010 (2009).
 - ¹⁹ E. Romera, J. B. Roldan, F. de los Santos, *Phys. Lett. A* **378**, 2582 (2014).
 - ²⁰ J. Cserti and G. David, *Phys. Rev. B* **74**, 172305 (2006).
 - ²¹ R. Winkler, U. Zulicke, and J. Bolte, *Phys. Rev. B* **75**,

- 205314 (2007).
- ²² T. O. Wehling, A. M. Black-Schaffer, and A. V. Balatsky, *Adv. in Phys.* **63**, 1 (2014).
- ²³ M. Studer, G. Salis, K. Ensslin, D. C. Driscoll, and A. C. Gossard, *Phys. Rev. Lett.* **103**, 027201 (2009).
- ²⁴ J. Nitta, T. Akazaki, H. Takayanagi, and T. Enoki, *Phys. Rev. Lett.* **78**, 1335 (1997).
- ²⁵ R. Winkler, *Phys. Rev. B* **62**, 4245 (2000).
- ²⁶ R. Winkler, *Spin-orbit Coupling Effects in Two-Dimensional Electron and Hole Systems* (Springer, Berlin, 2003).
- ²⁷ J. Schliemann and D. Loss, *Phys. Rev. B* **71**, 085308 (2005).
- ²⁸ B. A. Bernevig and S. C. Zhang, *Phys. Rev. Lett.* **95**, 016801 (2005).
- ²⁹ H. Nakamura, T. Koga, and T. Kimura, *Phys. Rev. Lett.* **108**, 206601 (2012).
- ³⁰ A. D. Caviglia, S. Gariglio, C. Cancellieri, B. Sacepe, A. Fete, N. Reyren, M. Gabay, A. F. Morpurgo, and J.M. Triscone, *Phys. Rev. Lett.* **105**, 236802 (2010).
- ³¹ K. S. Novoselov, A. K. Geim, S. V. Morozov, D. Jiang, Y. Zhang, S. V. Dubonos, I. V. Grigorieva, and A. A. Firsov, *Science* **306**, 666 (2004). K. S. Novoselov, A. K. Geim, S. V. Morozov, D. Jiang, M. I. Katsnelson, I. V. Grigorieva, S. V. Dubonos, and A. A. Firsov, *Nature* **438**, 197 (2005).
- ³² A. H. Castro Neto, F. Guinea, N. M. R. Peres, K. S. Novoselov, and A. K. Geim, *Rev. Mod. Phys.* **81**, 109 (2009).
- ³³ M.I. Katsnelson, *Graphene: Carbon in Two Dimensions*, (Cambridge University Press, Cambridge, 2012).
- ³⁴ K. Takeda and K. Shiraishi, *Phys. Rev. B* **50**, 14916 (1994). G. G. Guzmán-Verri and L. C. Lew Yan Voon, *Phys. Rev. B* **76**, 075131 (2007).
- ³⁵ B. Lalmi, H. Oughaddou, H. Enriquez, A. Kara, S. Vizzini, B. Ealet, B. Aufray, *Appl. Phys. Lett.* **97**, 223109 (2010). P. Vogt, P. De Padova, C. Quaresima, J. Avila, E. Frantzeskakis, M. C. Asensio, A. Resta, B. Ealet, and G. Le Lay, *Phys. Rev. Lett.* **108**, 155501 (2012).
- ³⁶ F. Bechstedt, L. Matthes, P. Gori and O. Pulci, *Appl. Phys. Lett.* **100**, 261906 (2012).
- ³⁷ S. Cahangirov, M. Audiffred, P. Tang, A. Iacomino, W. Duan, G. Merino, and A. Rubio *Phys. Rev. B* **88**, 035432 (2013).
- ³⁸ L. Chen, C.-C. Liu, B. Feng, X. He, P. Cheng, Z. Ding, S. Meng, Y. Yao, and K. Wu, *Phys. Rev. Lett.* **109**, 056804 (2012).
- ³⁹ S. Cahangirov, M. Topsakal, E. Aktürk, H. Sahin, and S. Ciraci, *Phys. Rev. Lett.* **102**, 236804 (2009).
- ⁴⁰ Z. Ni, Q. Liu, K. Tang, J. Zheng, J. Zhou, R. Qin, Z. Gao, D. Yu, and J. Lu, *Nano Lett.* **12**, 113 (2012).
- ⁴¹ D. Xiao, G.-B. Liu, W. Feng, X. Xu, and W. Yao, *Phys. Rev. Lett.* **108**, 196802 (2012).
- ⁴² M. Chhowalla, H. S. Shin, G. Eda, L.-J. Li, K. P. Loh and H. Zhang, *Nat. Chem.* **5**, 263 (2013).
- ⁴³ F. Rose, M. O. Goerbig, and F. Piechon, *Phys. Rev. B* **88**, 125438 (2013).
- ⁴⁴ X. Xu, W. Yao, Di Xiao, and T. F. Heinz, *Nat. Phys.* **10**, 343 (2014).
- ⁴⁵ T. M. Rusin and W. Zawadzki, *J. Phys.: Condens. Matter* **26**, 215301 (2014).
- ⁴⁶ M. Nauenberg, *J. Phys. B: At. Mol. Opt. Phys.* **23**, L385 (1990).
- ⁴⁷ V. Y. Demikhovskii, G. M. Maksimova, A. A. Perov, and A. V. Telezhnikov, *Phys. Rev. A* **85**, 022105 (2012).
- ⁴⁸ E. I. Rashba, *Sov. Phys. Solid State* **2**, 1109 (1960), Y. A. Bychkov and E. I. Rashba, *J. Phys. C: Solid State Phys.* **17**, 6039 (1984).
- ⁴⁹ X. F. Wang and P. Vasilopoulos, *Phys. Rev. B* **67**, 085313 (2003).
- ⁵⁰ R. Winkler, S. J. Papadakis, E. P. De Poortere, and M. Shayegan, *Phys. Rev. Lett.* **85**, 4574 (2000).
- ⁵¹ Z. Zhong, A. Toth, and K. Held, *Phys. Rev. B* **87**, 161102(R) (2013).
- ⁵² M. Zarea and S. E. Ulloa, *Phys. Rev. B* **73**, 165306 (2006).
- ⁵³ T. Ma and Q. Liu, *Appl. Phys. Lett.* **89**, 112102 (2006).